Metals as Ligands

International Edition: DOI: 10.1002/anie.201504414
German Edition: DOI: 10.1002/ange.201504414

The Mo–Mo Quintuple Bond as a Ligand to Stabilize Transition-Metal Complexes**

*Duan-Yen Lu, Peter P.-Y. Chen, Ting-Shen Kuo, and Yi-Chou Tsai**

Abstract: *Herein, we report the employment of the Mo–Mo quintuple bonded amidinate complex to stabilize Group 10 metal fragments* $\{(Et_3P)_2M\}$ *(M = Pd, Pt) and give rise to the isolation of the unprecedented δ complexes. X-ray analysis unambiguously revealed short contacts between Pd or Pt and two Mo atoms and a slight elongation of the Mo–Mo quintuple bond in these two compounds. Computational studies show donation of the Mo–Mo quintuple-bond δ electrons to an empty σ orbital on Pd or Pt, and back-donation from a filled Pd or Pt* d_π *orbital into the Mo–Mo δ* level (LUMO), consistent with the Dewar–Chatt–Duncanson model.*

Metal σ and π complexes are important species in metal-mediated synthesis and catalysis, in which the initial step usually involves the activation of chemical bonds of substrates by coordination to a metal fragment.[1] For example, in many hydrogenation and hydrogenolysis reactions, the metal dihydrogen σ complexes have been proposed the key intermediates, and confirmed by the characterization of the first isolable metal dihydrogen σ complexes $[M(CO)_3(PR_3)_2(\eta^2\text{-}H_2)]$ (M = Mo, W) by Kubas et al.[2] Moreover, the metal alkane σ complexes have been suggested to be the critical intermediates in C–H activation processes.[3,4] As for π complexes, since the identification of Zeise's salt $K[Pt(\eta^2\text{-}C_2H_4)Cl_3]$,[5] a very large number of π complexes contain π-bound organic groups acting as side-on bound ligands have been documented. In π complexes, the π type of ligands undergo umpolung reactions: olefins and alkynes in their free state are susceptible to electrophilic attack, but are inverted to nucleophilic attack upon coordination to transition metal centers.[6]

Metal–metal multiple bonds of the transition elements are redox active,[7] but activation of metal–metal multiple bonds by coordination to transition metals has not been explored. Though a large number of metal–metal triply and quadruply bonded dinuclear complexes have been reported,[8] their multiply bonded bimetallic centers are well shielded by supporting ligands from ligating to metal fragments. However, the metal–metal multiple bonding was recently reinvigorated by the discovery of the first quintuple bonded chromium dimer by Power et al. in 2005.[9] Since then, many quintuple bonded homounivalent Group VI dinuclear compounds containing nitrogen donors were subsequently characterized.[10] Preliminary reactivity examinations on these low-coordinate dinuclear species revealed that the presence of δ-bond charge density enable them to react with small inorganic molecules[11] and organic functionalities.[11,12] For example, these species underwent reductive complexation with the pnictogen elements[13a] and unsaturated hydrocarbons.[13b–d] Of particular interest is that, like unsaturated hydrocarbons, they underwent electrophilic addition reactions. For instance, Kempe et al. demonstrated an amidopyridine-stabilized quintuple-bonded dichromium complex underwent addition reactions with halogen and chalcogen elements,[14a] and $AlMe_3$ to give an interesting carboaluminated complex, *trans*-$[Cr_2(\mu\text{-}Me)[\mu\text{-}AlMe_2](\mu\text{-}AP)_2]$ (AP = amidopyridine).[14b] We reported the quintuple-bonded dimolybdenum amidinates $[\{Mo(\mu\text{-}\kappa^2\text{-}RC(N\text{-}2,6\text{-}i\mathrm{Pr}_2C_6H_3)_2)_2\}_2]$ (**1**: R = H, **2**: R = Ph)[10a,f] underwent Lewis acid-free Friedel–Crafts type of addition (or oxidative addition) with various acyl halides.[14c] In addition, both **1** and **2** underwent interesting catalyst-free [2+2+2] cycloadditions with terminal alkynes.[13d] In these examples, the quintuple-bonded dinuclear units served as two-electron reductants by losing one δ-bonding pair electrons, and, consequently, the formal metal–metal bond orders decrease from 5 to 4, accompanied by lengthening of the metal–metal bond.

The aforementioned reaction patterns suggests the nucleophilic nature of the metal–metal quintuple bonds. Accordingly we wondered if the quintuple-bonded complexes could serve as ligands and coordinate to metal fragments through donation of their δ-bonding electrons. This notion is further supported by their frontier orbitals which are topologically similar to acetylene and **1** as illustrated in Figure S1 in the Supporting Information. The HOMO (Mo–Mo δ) and HOMO−1(Mo–Mo δ) of **1** can donate electrons to a metal center in a π and σ fashion, respectively, while the LUMO (Mo–Mo δ*) can accept electron density from the metal center by π back-bonding. The two recently characterized paddlewheel complexes, $[Cr_2(\mu\text{-}Me)\{\mu\text{-}Al(CH_3)_2\}(\mu\text{-}AP)_2]$[14b] and $[(\mu\text{-}Li)Mo_2\{\mu\text{-}HC(N\text{-}2,6\text{-}Et_2C_6H_3)_2\}_3]$,[10d] where the former have both -$AlMe_2$ and -Me groups spanning the Cr–Cr quadruple bond, and the latter "-ate" species have

---

[*] Dr. D.-Y. Lu, Prof. Dr. Y.-C. Tsai
Department of Chemistry and Frontier Research Center on Fundamental and Applied Sciences and Matters
National Tsing Hua University
101, Sec. 2, Guang-Fu Road, Hsinchu 300 (Taiwan)
E-mail: yictsai@mx.nthu.edu.tw

Prof. Dr. P. P.-Y. Chen
Department of Chemistry, National Chung Hsing University
250, Kuo-Kuang Road, Taichung 402 (Taiwan)

T.-S. Kuo
Department of Chemistry, National Taiwan Normal University
88, Sec. 4, Ting-Chow Rd, Taipei 116 (Taiwan)

[**] We thank the Ministry of Science and Technology (Taiwan) and the Frontier Research Center on Fundamental and Applied Sciences of Matters of National Tsing Hua University for financial support.

Supporting information for this article is available on the WWW under http://dx.doi.org/10.1002/anie.201504414.

a lithium atom bridging a quintuple bonded Mo_2 unit, could be formally thought of as being δ complexes. However, the interactions in Al–Cr_2 and Li–Mo_2 are σ bonding only. Herein, we report the synthesis and characterization of the first examples of δ complexes, in which the Group 10 metal fragments $\{M(PEt_3)_2\}$ (M = Pd, Pt) are stabilized by a bulky ligand, the quintuple-bonded dimolybdenum amidinate, and the δ bonding between M and Mo_2 is confirmed by theoretical calculations.

As illustrated in Scheme 1, upon mixing **1** and the Group 10 metal complexes $[M(PEt_3)_n]$ (M = Pd, $n = 3$; M = Pt, $n = 4$), phosphine ligands of the Group 10 metal were readily replaced by **1** to give two δ complexes $[(Et_3P)_2M([Mo(\mu\text{-}HC(N\text{-}2,6\text{-}iPr_2C_6H_3)_2)_2]_2)]$ (**5**: M = Pd, **6**: M = Pt). It is noteworthy that the preparation of Group 10 metal δ complexes is not facile. For example, no reactions were observed between $[M(PEt_3)_n]$ and the bulkier quintuply bonded dimolybdenum amidinate **2**. Moreover, dichromium metal–metal quintuple bonding analogue of **1**, $[\{Cr(\mu\text{-}HC(N\text{-}2,6\text{-}iPr_2C_6H_3)_2)_2\}_2]$ (**3**)[10g] and the less sterically congested dichromium amidinate $[\{Cr(\mu\text{-}HC(N\text{-}2,6\text{-}Et_2C_6H_3)_2)_2\}_2]$ (**4**)[10g] do not displace the phosphine ligands of $[M(PEt_3)_n]$.

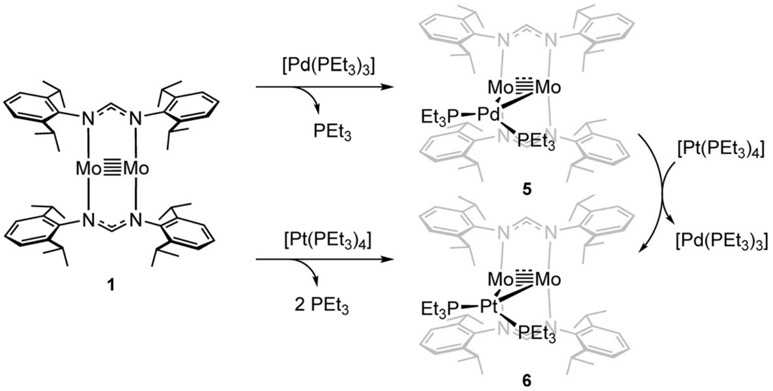

Scheme 1. Preparation of complexes **5** and **6**.

Both **5** and **6** are thermally robust, but are extremely air and moisture sensitive. Their solids can be stored at room temperature under a dinitrogen atmosphere for a long period without decomposition. However, they display different behavior in solutions. Complex **6** is stable in hydrocarbon solvents, but **5** quickly decomposes to give $\{(Et_3P)_2Pd\}$ and **1** upon dissolution in organic solvents, particularly in coordinating solvents, such as benzene, toluene, and tetrahydrofuran (THF), which was further corroborated by UV/Vis spectroscopy (Figure S2). Therefore, **6** can be alternatively prepared by mixing **5** and an equimolar amount of $[Pt(PEt_3)_4]$ in n-hexane. The facile metal-substitution reaction suggests the formulation of **5** and **6** as species resulting from a Lewis acid/base interaction between the $\{M(PEt_3)_2\}$ fragment and the Mo–Mo quintuple bond of **1**.

Both ^1H and ^{31}P NMR spectra of **5** (in $[D_{12}]$cyclohexane) and **6** (in $[D_6]$benzene) revealed one set of amidinate and phosphine ligand signals, indicating two-fold symmetry. The single ^{31}P NMR resonance signal (**5**: $\delta = 15.2$ ppm, **6**: $\delta = 35.7$ ppm) of **6** showed a ^{195}Pt–^{31}P ($^1J_{PtP}$) coupling constant of 3298 Hz, coincidently in the range of $^1J_{PtP}$ values of 3160–3443 Hz in the $[(Et_3P)_2Pt(\pi\text{-alkyne})]$ complexes.[15] The $^1J_{PtP}$ values are associated with the valency of the Pt centers in complexes $cis\text{-}[(Et_3P)_2PtL_2]$. The divalent platinum dialkyl complexes display $^1J_{PtP}$ values less than 2000 Hz, while the zero-valent Pt π complexes $[(Et_3P)_2Pt(\pi\text{-alkyne})]$ and $[(Et_3P)_2Pt(\pi\text{-alkene})]$ have larger $^1J_{PtP}$ values in the range of 3460-3663 Hz.[15] In addition, $^1J_{PtP}$ has been an indispensable diagnostic parameter to differentiate between $[(Et_3P)_2Pt(\pi\text{-alkyne})]$ and $[(Et_3P)_2Pt(\pi\text{-alkene})]$, because the π-alkyne complexes usually have stronger Pt to C–C π* back-donation than the π-alkene, and, therefore, exhibit smaller $^1J_{PtP}$ values by 100–300 Hz.[15] As a result, Pt centers in **6** and $[(Et_3P)_2Pt(\pi\text{-alkyne})]$ complexes have comparable electronic properties and valency. Notably, since the π-alkyne complexes of $\{(Et_3P)_2Pd\}$ have not been reported, no relevant structural parameters can be compared to **5**.

X-ray crystallography was used to study the molecular structures of **5** and **6**. Interestingly, two different unit cells of **5** were obtained upon recrystallization in diethyl ether at −35 °C and n-hexane at room temperature. At low temperature, the unit cell contained two molecules of **5**, while it unexpectedly consisted of two molecules of **5** and one molecule of **1** (2**5**·**1**) at room temperature. The X-ray structures of compounds **5** and **6** are depicted in and Figure 1, while 2**5**·**1** has a highly disordered molecule **1**, so is shown in Figure S3. The planar P_2MMo_2 cores of **5** and **6** are

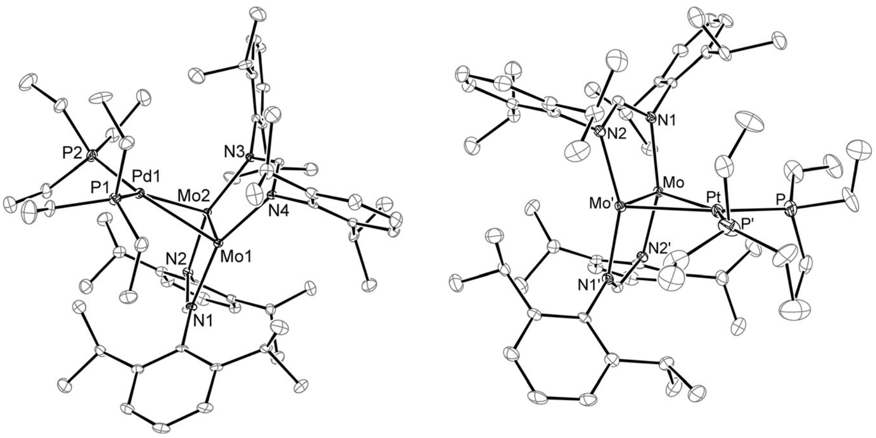

Figure 1. The solid-state molecular structures of left: **5** and right: **6** determined by X-ray crystallography. Thermal ellipsoids set at 35 % probability. Hydrogen atoms have been omitted for clarity. Selected bond lengths [Å] and angles [°]: **5**: Pd1-Mo1 2.7200(11), Pd1-Mo2 2.7168(10), Mo1-Mo2 2.0557(8); dihedral Mo1/Mo2/P2/P1, 7.34(4). **6:** Mo-Pt 2.6750(5), Mo-Mo′ 2.0728(8); dihedral Mo/Mo′/P′/P 4.32(5).

identical to those planar P_2PtC_2 in the complexes of $[(PEt_3)_2Pt(\pi\text{-alkyne})]$,[16] showing that the immediate coordination sphere of Pd and Pt displays a square-planar geometry, taking the two phosphorus atoms and two molybdenum atoms as coordinating atoms, with parallel P–P and Mo–Mo axes. In addition to the $^1J_{PtP}$ values, the P-Pt-P angles in *cis*-$[(Et_3P)_2PtL_2]$ also divulge the valency of Pt. In the divalent platinum dialkyl complexes, the P-Pt-P angles are in the range of 94 and 106°, whereas the P-Pt-P angles of the Pt π-olefin and π-alkyne complexes range from 100 to 108°.[15] In **5** and **6**, the P-M-P bond angles are greater than 108° but decrease in the order **5** (116.72 (6)°) > **6** (108.34(11)°). The valency of Pt in **6** is comparable with those of π-alkyne complexes $[(Et_3P)_2Pt(\pi\text{-alkyne})]$. Another interesting parallel structural feature of **5** and **6** with $[(Et_3P)_2Pt(\pi\text{-alkyne})]$ is that both amidinate ligands also bend back away from the Pd and Pt centers by about 11.8° and 12.8°, respectively, much smaller than that of the 3-hexyne-coordinated **2** (ca. 25°), which features a formal Mo–Mo quadruple bond.[13d] The Pd–Mo bond lengths, 2.7200(11) and 2.7168(10) Å in **5** are longer than two crystallographically identical Pt–Mo bond of 2.6750(5) Å in **6**. Since the covalent radius of Pd (1.283 Å) and Pt (1.295 Å) are almost equivalent,[17] **1** is thus bound more strongly to Pt than to Pd, which is consistent with their different stability in solution. The Mo–Mo bond length of 2.0728(8) Å in **6** is slightly longer than that of **5** (2.0557(8) Å), which are respectively lengthened by 1.8 and 1.7%, compared with the Mo–Mo quintuple bond length of 2.0187(9) Å in **1**.[10f]

In the π complexes $[(R_3P)_2M(\pi\text{-olefin})]$ and $[(R_3P)_2M(\pi\text{-alkyne})]$ (M = Pd, Pt), the π back-bonding from a filled d orbital of M to the π* orbitals of alkenes or alkynes plays a crucial role to the geometries of the central planar P_2MC_2 cores. The planar P_2MMo_2 array in **5** and **6** suggests similar bonding interactions between the $\{M(PEt_3)_2\}$ and dimolybdenum fragments. To delineate their bonding schemes and the nature of the Mo–Mo bond in **5** and **6**, Kohn–Sham density functional theory (DFT) calculations at the BP86/def2-TZVP level were undertaken of **5** and **6** without simplification of groups. To compare with the corresponding π-alkyne complexes of $\{(Et_3P)_2Pt\}$ we also calculated the hypothetical π-alkyne compound $[(Et_3P)_2Pt(\eta^2\text{-}C_2H_2)]$ by using the same method. The theoretically calculated bond-dissociation energy (BDE), that is, the difference between the energy summation of **1** and $\{M(PEt_3)_2\}$ in their singlet ground state and the energy of **5** and **6**, was 5.1 (M = Pd) and 10.7 kcal mol^{-1} (for M = Pt), while that of $[(Et_3P)_2Pt(\eta^2\text{-}C_2H_2)]$ was 21.5 kcal mol^{-1} (M = Pt). These calculated BDEs are consistent with the labile behavior of the complexes in solutions and with the trend of the hypothetical π-alkyne complexes $[(Me_3P)_2M(\eta^2\text{-}C_2H_2)]$ (M = Pd, Pt).[18] The computed Pt-Mo (2.725 Å) and Mo-Mo (2.081 Å) bond lengths were only slightly longer than the experimental values, which can be explained by the influence of molecular packing in the solid state. It has been shown that donor–acceptor bonds in the solid state are shorter than in the gas phase, mainly because of intermolecular interactions.[19] Note that although the steric crowding at the Pt center in **6** is much greater than that of $[(Et_3P)_2Pt(\eta^2\text{-}C_2H_2)]$, the calculated P-Pt-P angles are differ little, 112.04 and 112.16°, respectively, indicating comparable valency of Pt in both compounds.

A fragment molecular orbital approach was then used to analyze the bonding between the dimolybdenum unit and the Pt atom in **6** (roughly C_{2v} symmetry; Figure 2), and the bonding between two C atoms and the Pt center in $[(Et_3P)_2Pt(\eta^2\text{-}C_2H_2)]$ (Figure S5). Their fragment electronic structures were obtained from single-point energy calculations without geometry optimization on the fragment coordinates obtained from calculations giving converged geometries for the complete molecules of **6** and $[(Et_3P)_2Pt(\eta^2\text{-}C_2H_2)]$. The filled Mo_2 fragment a_1 (the lower δ orbital) interacts with $1a_1$ and $3a_1$ of $\{Pt(PEt_3)_2\}$ to produce three MOs; the highest occupied one

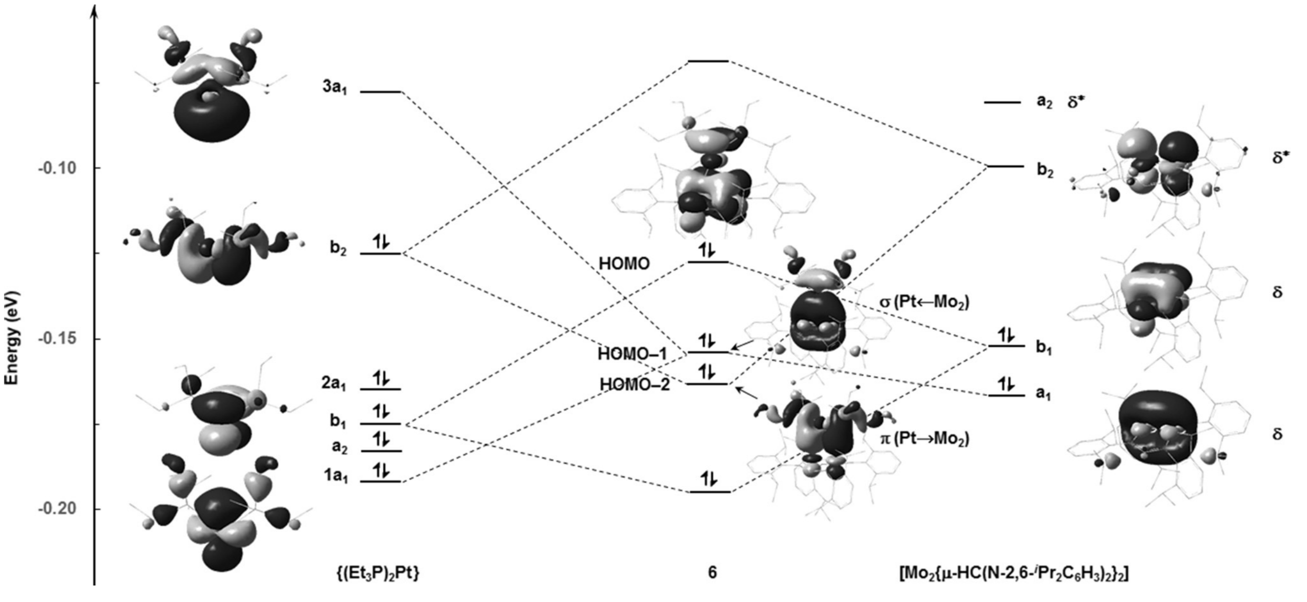

Figure 2. An orbital interaction diagram for complex **6**.

(Pt–Mo_2 σ bonding, HOMO−1) is shown in Figure 2. The occupied Mo_2 fragment b_1 (the higher δ orbital) overlaps with the filled $1b_1$ of {$Pt(PEt_3)_2$} to give two occupied molecular orbitals, which cancel each other with respect to Pt–Mo_2 π bonding. The a_2 and $2a_1$ orbitals of {$Pt(PEt_3)_2$} are nonbonding. The combination of the filled b_2 of {$Pt(PEt_3)_2$} and the empty b_2 (the lowest δ* orbital) of the Mo_2 group is Pt to Mo_2 back-bonding and gives rise to the formation of a strong π-bonding interaction. As a result, this synergistic δ-bonding scheme can be described by Dewar–Chatt–Duncanson model.[20] Significant preservation of two Mo–Mo δ bonds in **6** was observed at its HOMO and HOMO−1, which display a large component of Mo–Mo δ-bonding orbitals (58 and 63 %, respectively). The HOMO−2 consists of 27 % of a filled Pt d–p hybridized orbital and 27 % of the δ* orbital of the Mo_2 unit. Accordingly, their M–Mo_2 bonding situation of **5** and **6** is described to lie between the two extreme forms, namely, the side-on complex and metallacycle.

Quantifications of the Mo_2 to M σ and M to the Mo_2 π contributions to the stability of **5** and **6** were made by the extended transition state-natural orbital for chemical valence (ETS-NOCV) formalism implemented in Amsterdam density functional program.[21] These are amounted to −11.2 (σ) and −24.6 (π) $kcal\,mol^{-1}$ for **5** and −13.5 (σ) and −28.1 (π) kcal mol^{-1} for **6** (Figure S4). Additionally, the DFT-calculated Mulliken atomic charges of Mo atoms showed a decrease from 0.22 of **1** to −0.20 in **6** and an increase to 0.35 and 0.49 in **5**. The difference in the Mo atomic charges between **5** and **6** is possibly because of the greater π basicity of Pt than Pd, owing to the relativistically induced diffuseness and higher energy of the metal d-type donor orbital. As a result, **5** has a weaker back-bonding interaction from the Pd center to the Mo_2 unit. Moreover, the electron-density loss from the Mo_2 unit to Pd by σ electron donation and from two amidinate ligands to Mo_2 owing to structural distortion, contributed to the increase of Mo atomic charges. Similar trends in the atomic-charge variation were also observed in the hypothetical complex [$(Et_3P)_2Pt(\eta^2\text{-}C_2H_2)$], whereby the charge of Pt is 0.08, and that of C of the acetylene ligand is −0.31, while it is −0.19 in the free acetylene.

In view of the tetrahedral coordination of the Al center in [Cr_2(μ-Me)[μ-Al(CH_3)$_2$](μ-AP)$_2$], we wondered why **5** and **6** favor the conformation with the Mo–Mo axis parallel to the P–P axis (Figure 3 a), instead of being perpendicular to it (Figure 3 b). Attempts to optimize the perpendicular conformation of **6** by DFT calculations at the BP86/def2-TZVP level unequivocally led to the parallel structure. Is the structural preference for the parallel orientation resulted from electronic or steric effects? Optimization of the model compound [$(Me_3P)_2Pt${Mo(μ-HC($NMe)_2$)}$_2$] by the same method indicated that the perpendicular structure does not exist (Figure S7). Notably, the core structural parameters of the optimized model compound are very close to those of the calculated **6**. It is thus apparent that the structural orientation of **5** and **6** is predominantly controlled by the bonding interactions between Mo_2 and Pt. The conformational preference of **5** and **6** can be interpreted by examining their frontier orbital interactions between the {$(Et_3P)_2M$} and {Mo_2} fragments. Figure S6 shows orbital interaction diagrams for **5** and **6** in the two possible orientations. In both conformations, $1a_1$ and $3a_1$ of {$(Et_3P)_2M$} interact with a_1 (δ orbital) of [Mo_2{μ-HC(N-2,6-*i*$Pr_2C_6H_3)_2$}$_2$] to give rise to the formation of three molecular orbitals. Notably, the overlap between these three fragment orbitals is essentially invariant to rotation, because all are cylindrically symmetrical with respect to the M–Mo_2 axis. It is thus clear that the conformation of **5** and **6** is dominated by the $(Et_3P)_2M$–Mo_2 π bonding. In the perpendicular conformation as shown on the left side of Figure *S*6, the b_2 orbital of {$M(PEt_3)_2$} is destabilized upon overlap with the filled [Mo_2{μ-HC(N-2,6-*i*$Pr_2C_6H_3)_2$}$_2$] b_2 level (δ orbital). The two occupied molecular orbitals then cancel each other out. When the [Mo_2{μ-HC(N-2,6-*i*$Pr_2C_6H_3)_2$}$_2$] ligand is rotated by 90° to the parallel conformation on the right side of Figure *S*6, the δ* orbital is transformed into b_2 symmetry. The {$M(Et_3P)_2$} b_2 level is then greatly stabilized upon overlap with the [Mo_2{μ-HC(N-2,6-*i*$Pr_2C_6H_3)_2$}$_2$] b_2 fragment. In other words, the b_2 orbital of the Mo_2 fragment is able to accept back-bonding form the M center. To maximize the overlap with b_2 of {$M(PEt_3)_2$}, the Mo_2 unit must be coplanar with the P_2Pt plane, because both energy gap and overlap factors make the interaction between b_2 and δ* stronger than that for $b_1 + \delta^*$.

An absolute quantification of the Mo–Mo bond orders of **5** and **6** were made by analyzing the Mayer bond order of 3.79 (**5**) and 3.92 (**6**), which are slightly lower than the 4.24 of **1**, but higher than the calculated Cr–Cr bond order of approximately 3.6 in Power's quintuple bonded dichromium complexes.[22] On the other hand, the computed Mayer bond order of the C−C bond of the bound acetylene ligand in [$(Et_3P)_2Pt(\eta^2\text{-}C_2H_2)$] was 2.08 accompanied by its bond length of 1.296 Å (lengthening 6.8 %), while the corresponding values of the C−C bond in free C_2H_2 were 2.97 and 1.208 Å, respectively. In light of the short Mo–Mo distances and large Mayer bond orders in **5** and **6**, the formulation of the Mo–Mo bonds in both **5** and **6** formally as quintuple bonds seems reasonable as is the formal C–C triple bond of the C_2H_2 ligand in [$(Et_3P)_2Pt(\eta^2\text{-}C_2H_2)$].

In summary, we have demonstrated that, like H_2 σ and C_2H_4 π bonds, the Mo–Mo quintuple bond of **1** can serve as a ligand, which can substitute phosphine ligands in [$M(PEt_3)_x$] (M = Pd, Pt) to give the unprecedented metal δ-complexes **5** and **6**. Experiments and computations unequivocally corroborate the existence of δ bonding between the {$M(PEt_3)_2$} and quintuple-bonded dimolybdenum fragments. This work suggests that activation of the metal–metal δ bonds could be made possible by ligation to transition-metal fragments.

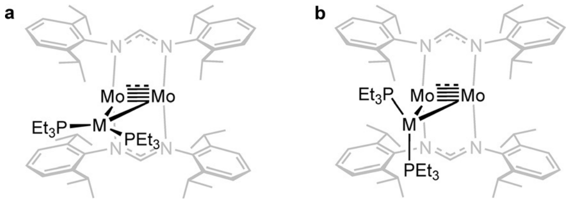

Figure 3. Two possible conformations of **5** and **6**.

Keywords: bonding · Group 10 metals · molybdenum · δ-bond · δ-complex

How to cite: *Angew. Chem. Int. Ed.* **2015**, *54*, 9106–9110
Angew. Chem. **2015**, *127*, 9234–9238

---

[1] R. H. Crabtree, *The Organometallic Chemistry of The Transition Metals*, Wiley, Hoboken, **2009**.

[2] G. J. Kubas, R. R. Ryan, B. I. Swanson, P. J. Vergamini, H. J. Wasserman, *J. Am. Chem. Soc.* **1984**, *106*, 451–452.

[3] a) J. A. Labinger, J. E. Bercaw, *Nature* **2002**, *417*, 507–514; b) W. D. Jones, *Inorg. Chem.* **2005**, *44*, 4475–4484; c) B. A. Arndtsen, R. G. Bergman, T. A. Mobley, T. H. Peterson, *Acc. Chem. Res.* **1995**, *28*, 154–162.

[4] a) S. D. Pike, A. L. Thompson, A. G. Algarra, D. C. Apperley, S. A. Macgregor, A. S. Weller, *Science* **2012**, *337*, 1648–1651; b) W. H. Bernskoetter, C. K. Schauer, K. I. Goldberg, M. Brookhart, *Science* **2009**, *326*, 553–556; c) I. Castro-Rodriguez, H. Nakai, P. Gantzel, L. N. Zakharov, A. L. Rheingold, K. Meyer, *J. Am. Chem. Soc.* **2003**, *125*, 15734–15735; d) D. R. Evans, T. Drovetskaya, R. Bau, C. A. Reed, P. D. W. Boyd, *J. Am. Chem. Soc.* **1997**, *119*, 3633–3634.

[5] a) W. C. Zeise, *Ann. Phys. Chem.* **1831**, *97*, 497–541; b) J. A. J. Jarvis, B. T. Kilbourn, P. G. Owsten, *Acta Crystallogr. Sect. B* **1971**, *B27*, 366–372.

[6] A. Fürstner, P. W. Davies, *Angew. Chem. Int. Ed.* **2007**, *46*, 3410–3449; *Angew. Chem.* **2007**, *119*, 3478–3519.

[7] M. H. Chisholm, *Chem. Rec.* **2001**, *1*, 12–23.

[8] F. A. Cotton, L. A. Murillo, R. A. Walton, *Multiple Bond Between Metal Atoms*, 3rd ed., Springer, Berlin, **2005**.

[9] T. Nguyen, A. D. Sutton, S. Brynda, J. C. Fettinger, G. J. Long, P. P. Power, *Science* **2005**, *310*, 844–847.

[10] a) M. Carrasco, N. Curado, C. Maya, R. Peloso, A. Rodríguez, E. Ruiz, S. Álvarez, E. Carmona, *Angew. Chem. Int. Ed.* **2013**, *52*, 3227–3231; *Angew. Chem.* **2013**, *125*, 3309–3313; b) L. J. Clouston, R. B. Siedschlag, P. A. Rudd, N. Planas, S. Hu, A. D. Miller, L. Gagliardi, C. C. Lu, *J. Am. Chem. Soc.* **2013**, *135*, 13142–13148; c) A. Noor, T. Bauer, T. K. Todorova, B. Weber, L. Gagliardi, R. Kempe, *Chem. Eur. J.* **2013**, *19*, 9825–9832; d) S.-C. Liu, W.-L. Ke, J.-S. K. Yu, T.-S. Kuo, Y.-C. Tsai, *Angew. Chem. Int. Ed.* **2012**, *51*, 6394–6397; *Angew. Chem.* **2012**, *124*, 6500–6503; e) Y.-L. Huang, D.-Y. Lu, H.-C. Yu, J.-S. K. Yu, C.-W. Hsu, T.-S. Kuo, G.-H. Lee, Y. Wang, Y.-C. Tsai, *Angew. Chem. Int. Ed.* **2012**, *51*, 7781–7785; *Angew. Chem.* **2012**, *124*, 7901–7905; f) Y.-C. Tsai, H.-Z. Chen, C.-C. Chang, J.-S. K. Yu, G.-H. Lee, Y. Wang, T.-S. Kuo, *J. Am. Chem. Soc.* **2009**, *131*, 12534–12535; g) C.-W. Hsu, J.-S. K. Yu, C.-H. Yen, G.-H. Lee, Y. Wang, Y.-C. Tsai, *Angew. Chem. Int. Ed.* **2008**, *47*, 9933–9936; *Angew. Chem.* **2008**, *120*, 10081–10084; h) Y.-C. Tsai, C.-W. Hsu, J.-S. K. Yu, G.-H. Lee, Y. Wang, T.-S. Kuo, *Angew. Chem. Int. Ed.* **2008**, *47*, 7250–7253; *Angew. Chem.* **2008**, *120*, 7360–7363; i) A. Noor, F. R. Wagner, R. Kempe, *Angew. Chem. Int. Ed.* **2008**, *47*, 7246–7249; *Angew. Chem.* **2008**, *120*, 7356–7359; j) R. Wolf, C. Ni, T. Nguyen, M. Brynda, G. J. Long, A. D. Sutton, R. C. Fischer, J. C. Fettinger, M. Hellman, L. Pu, P. P. Power, *Inorg. Chem.* **2007**, *46*, 11277–11290; k) K. A. Kreisel, G. P. A. Yap, P. O. Dmitrenko, C. R. Landis, K. H. Theopold, *J. Am. Chem. Soc.* **2007**, *129*, 14162–14163.

[11] a) A. Noor, S. Schwarz, R. Kempe, *Organometallics* **2015**, *34*, 2122–2125; b) A. Noor, S. Qayyum, T. Bauer, S. Schwarz, B. Weber, R. Kempe, *Chem. Commun.* **2014**, *50*, 13127–13129; c) P.-F. Wu, S.-C. Liu, Y.-J. Shieh, T.-S. Kuo, G.-H. Lee, Y. Wang, Y.-C. Tsai, *Chem. Commun.* **2013**, *49*, 4391–4393; d) C. Ni, B. D. Ellis, G. J. Long, P. P. Power, *Chem. Commun.* **2009**, 2332–2334.

[12] a) A. Noor, R. Kempe, *Inorg. Chim. Acta* **2015**, *424*, 75–82; b) A. K. Nair, N. V. S. Harisomayajula, Y.-C. Tsai, *Inorg. Chim. Acta* **2015**, *424*, 51–62; c) A. K. Nair, N. V. S. Harisomayajula, Y.-C. Tsai, *Dalton Trans.* **2014**, *43*, 5618–5638; d) N. V. S. Harisomayajula, A. K. Nair, Y.-C. Tsai, *Chem. Commun.* **2014**, *50*, 3391–3412; e) S.-A. Hua, Y.-C. Tsai, S.-M. Peng, *J. Chin. Chem. Soc.* **2014**, *61*, 9–26; f) F. R. Wagner, A. Noor, R. Kempe, *Nat. Chem.* **2009**, *1*, 529–536.

[13] a) C. Schwarzmaier, A. Noor, G. Glatz, M. Zabel, A. Y. Timoshkin, B. M. Cossairt, C. C. Cummins, R. Kempe, M. Scheer, *Angew. Chem. Int. Ed.* **2011**, *50*, 7283–7286; *Angew. Chem.* **2011**, *123*, 7421–7424; b) J. Shen, G. P. A. Yap, K. H. Theopold, *Chem. Commun.* **2014**, *50*, 2579–2581; c) A. Noor, E. S. Tamne, B. Oelkers, T. Bauer, S. Demeshko, F. Meyer, F. W. Heinemann, R. Kempe, *Inorg. Chem.* **2014**, *53*, 12283–12288; d) H.-Z. Chen, S.-C. Liu, C.-H. Yen, J.-S. K. Yu, Y.-J. Shieh, T.-S. Kuo, Y.-C. Tsai, *Angew. Chem. Int. Ed.* **2012**, *51*, 10342–10346; *Angew. Chem.* **2012**, *124*, 10488–10492.

[14] a) E. S. Tamne, A. Noor, S. Qayyum, T. Bauer, R. Kempe, *Inorg. Chem.* **2013**, *52*, 329–336; b) A. Noor, G. Glatz, R. Muller, M. Kaupp, S. Domeshko, R. Kempe, *Nat. Chem.* **2009**, *1*, 322–325; c) H.-G. Chen, H.-W. Hsueh, T.-S. Kuo, Y.-C. Tsai, *Angew. Chem. Int. Ed.* **2013**, *52*, 10256–10260; *Angew. Chem.* **2013**, *125*, 10446–10450.

[15] H. Braunschweig, P. Brenner, R. D. Dewhurst, I. Krummenacher, B. Pfaffinger, A. Vargas, *Nat. Commun.* **2012**, 3:872 doi: 10.1038/ncomms1884.

[16] F. Bauer, H. Braunschweig, K. Gruss, T. Kupfer, *Organometallics* **2011**, *30*, 2869–2884.

[17] L. Pauling, *The Nature of the Chemical Bond and the Structure of Molecules and Crystals; an Introduction to Modern Structural Chemsitry*, 3rd ed., Cornell University Press, Ithaca, N.Y., **1960**.

[18] C. Massera, G. Frenking, *Organometallics* **2003**, *22*, 2758–2765.

[19] V. Jonas, G. Frenking, M. T. Reetz, *J. Am. Chem. Soc.* **1994**, *116*, 8741–8753.

[20] a) M. J. S. Dewar, *Bull. Soc. Chim. Fr.* **1951**, C71–C79; b) J. Chatt, L. A. Duncanson, *J. Chem. Soc.* **1953**, 2939–2947.

[21] a) M. P. Mitoraj, A. Michalak, T. Ziegler, *Organometallics* **2009**, *28*, 3727–3733; b) M. P. Mitoraj, A. Michalak, T. Ziegler, *J. Chem. Theory Comput.* **2009**, *5*, 962–975.

[22] M. Brynda, L. Gagliardi, P. O. Widmark, P. P. Power, B. O. Roos, *Angew. Chem. Int. Ed.* **2006**, *45*, 3804–3807; *Angew. Chem.* **2006**, *118*, 3888–3891.

Received: May 15, 2015